Multiple scattering measurements in optically dense media

Jin H. Park, C. Russell Philbrick
Department of Electrical Engineering, The Pennsylvania State University
University Park, 16802, State College, USA
jxp943@psu.edu, crp3@psu.edu

Abstract. Multiple scattering is an important factor in treating the penetration of radiation through an optically thick medium, such as clouds and fog. Numerical calculations are performed using a Bistatic Monte Carlo method, and compared with chamber and field experiments conducted under a range of atmospheric conditions. The radial distributions of radiation scattered from the multistatic lidar beam are analyzed using CCD images to measure the spatial characteristics of multiple scattering. Changes in the multiple scattering characteristics are related to the number and size of scatterers in terms of optical depth. The polarization ratio of the scattering phase function also proved to be a useful way to extract multiple scattering effects at particular scattering angles. Multiple scattering increases the depolarization at side-scattering region, smaller than 160°.

Keywords: multiple scattering, multistatic lidar, radial distribution, polarization ratio, fog.

1 INTRODUCTION

Sensing the multiple scattering of optically dense media can enhance lidar measurements by providing additional information on the microphysical properties of atmospheric aerosols. Multiple scattering is an often encountered phenomenon, which is important in treating the penetration of radiation through optically thick media such as clouds and fog. A multistatic lidar system, which was developed at the Pennsylvania State University, has an ability to evaluate multiple scattering effects by measuring polarization ratio of the scattering phase function at different scattering angles, as well as the radial distribution of the multiple scattering component from a transmitted laser beam. Measurements of aerosol properties as a function of scattering angle are particularly important for extracting information on the characteristics of the optical scatterers such as particle sizes and number density. It was also known that the width of the intensity peak is inversely proportional to the particle size when multiple scattering effects occur along the beam path [1].

Laboratory experiments were conducted in Aerosol Research Chamber in Defense Research and Development Canada (DRDC) in Quebec, and small chamber assembled at PSU to conduct scattering experiments in a better controlled environment. In addition, a set of outdoor field studies were performed in State College, Pennsylvania in the summer of 2007. The field experiments were made under conditions of sufficiently high relative humidity and fog that it is reasonable to use a spherical model to describe the scattering particles. These studies were conducted under perfect conditions to investigate multiple scattering effects. Numerical calculations of multiple scattering using a Bistatic Monte Carlo (BMC) method are compared with multiple scattering measurements.

2 EXPERIMENTAL

Experiments were conducted in a cooperative research project between researchers from The Pennsylvania State University and from Defense Research and Development Canada (DRDC).

The DRDC Aerosol Research Chamber provided an opportunity to investigate multiple scattering characteristics. The multistatic lidar measurements were made in a 22-m long aerosol chamber with a 2.4 m × 2.4 m cross-section that is located at the DRDC facility [2]. It has doors at the ends of the chamber that can be opened quickly to ensure a uniform distribution of particles inside the chamber, see Fig. 1 (a). The inside of the chamber is coated with optical-black paint to avoid reflecting light from the walls. A small chamber was also assembled at PSU to conduct scattering experiments in a better controlled laboratory environment using aerosols from a generator, and characterizing them with a size spectrometer and a particle counter. The PSU chamber is much smaller than that of the DRDC facility, however it is much easier to control particle characteristics in the chamber, see Fig. 1 (b). Outdoor field experiments were performed in State College, Pennsylvania in the summer of 2007. The field experiments were made under sufficiently high relative humidity and on heavy foggy night, which is reasonable to use a spherical model to describe scattering particles and perfect conditions to observe multiple scattering effects. The main aerosol type used in each chamber experiment was artificial fog disseminated by a MDG Super Max 5000 fog generator in the DRDC chamber, and a TDA-5A Aerosol generator in the PSU chamber. The size distribution of artificial fog was measured using a TSI 3934 SMPS. The particle size spectrometer measurements provided a well characterized log-normal size distribution. Fig. 2 shows the measured size distributions characteristic of the aerosols used for the two chamber tests. Each parameter of the best fit log-normal size distribution is tabulated in Table 1.

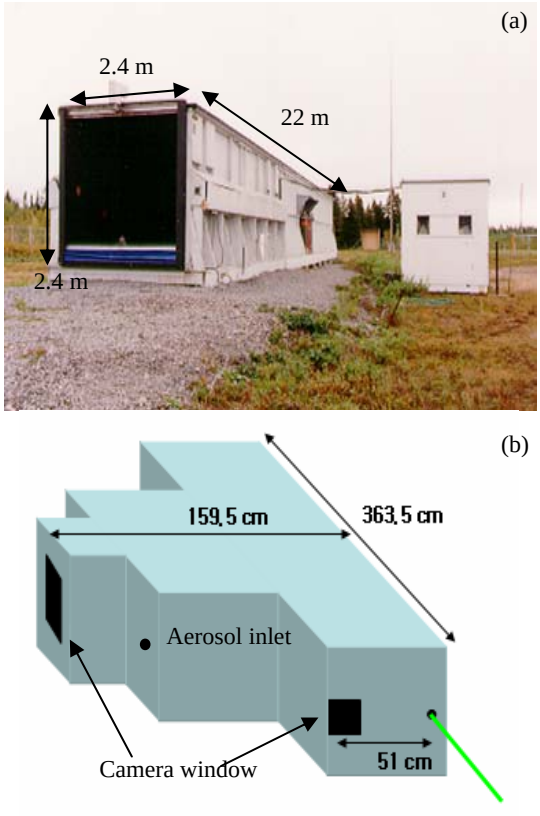

Fig. 1. Aerosol chambers of (a) DRDC and (b) PSU.

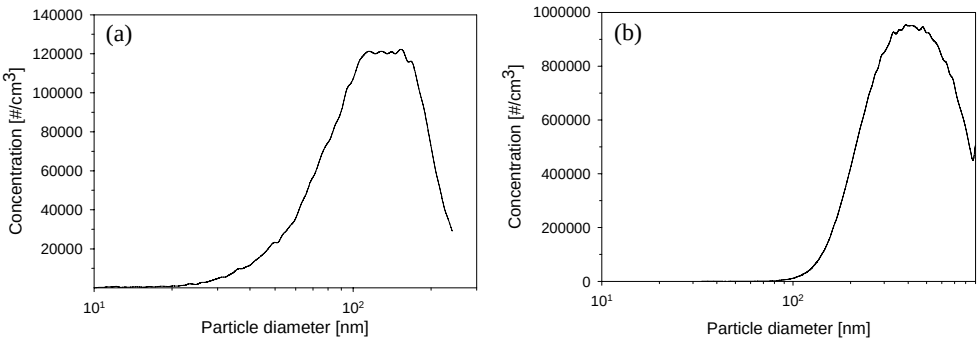

Fig. 2. Size distributions of artificial fog of (a) a MDG Super Max 5000 fog generator at DRDC chamber and (b) a TDA-5A aerosol generator at PSU small chamber.

Table 1. Parameters of the best fit size distribution and refractive index of fog.

Parameter	Fog oil (a)	Fog oil (b)
Median diameter [μm]	0.1176	0.317
Geo. St. Dev	1.71	1.66
Total Conc. [#/cm^3]	6.03×10^4	1.09×10^6
Refractive index	$1.51 + 0i$	$1.47 + 0i$

The optical setup of the multistatic lidar used for the measurements is shown in Fig. 3. The detailed setup of the system was also explained in a previous paper [3]. A CW Nd-VYO4 laser with a wavelength of 532 nm is used. The detectors are commercial CCD cameras fitted with wide field lenses (FOV approximately 48°). The choice of wide angle optics eliminates the need for spatial scanning to cover the desired range of scattering angles. The transmitter and two detectors were separated from the laser beam path and each detector was in line with the direction of the beam propagation. A polarization cube (Glan Taylor prism) and a 90° polarization rotator were used to separate laser beam into two orthogonally polarized components. The polarization rotator was controlled remotely by a mechanical device. During the experiments, measurements were made simultaneously in backward and forward scattering direction. Light scatter close to the forward direction is sensitive to size but rather insensitive to refractive index and particle shape [1,4]. Measurements of the polarization ratio in the backscattering direction (at angles < 175°) provide a useful experimental approach to observe the microphysical properties of aerosol particles [5-7].

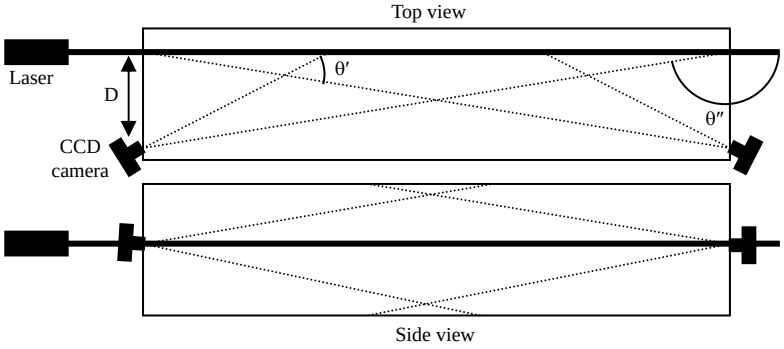

Fig. 3. Optical setup of the multistatic lidar receivers.

3 THEORY

The configuration of the bistatic lidar is shown in Fig. 4. The laser beam is transmitted in the horizontal direction and the detectors, which are separated from the laser by a distance D, can be located at both forward and backward directions, see Fig. 3. The received power from a scattered volume within unit angle, $d\alpha$, which is the field of view of one pixel, can be described as [8],

$$P_r = P_t \frac{KAT_t T_r \beta(z,\theta)}{R^2} dz \quad , \tag{1}$$

where P_r is the received power, P_t is the transmitted power, K is the optical efficiency of the detector, A is the collecting area of the detector, and T_t and T_r are the atmospheric transmittance from the transmitter to a scattering medium and from a scattering medium to the detector at range R, respectively, and $\beta(z,\theta)$ is the scattering coefficient, which is a function of range z and scattering angle θ. The scattering angle, θ, can be denoted as either θ' (in the forward direction) or θ'' (in the backward direction) in Fig. 3. The scattering angle is determined by the perpendicular distance between a transmitter beam and the detector, D, the location of the imaged pixel in the FOV of the detector, and the pointing direction of the detector. In case of a small-scale experiment, the transmittances, T_t and T_r are almost same.

The benefit of multistatic arrangement is that the received signal intensity does not depend strongly on the range, which is $1/R^2$ in the case of a conventional monostatic lidar system. From the geometry of Fig. 4, the range resolution dz is given simply by

$$dz = R^2 \frac{d\alpha}{D}. \tag{2}$$

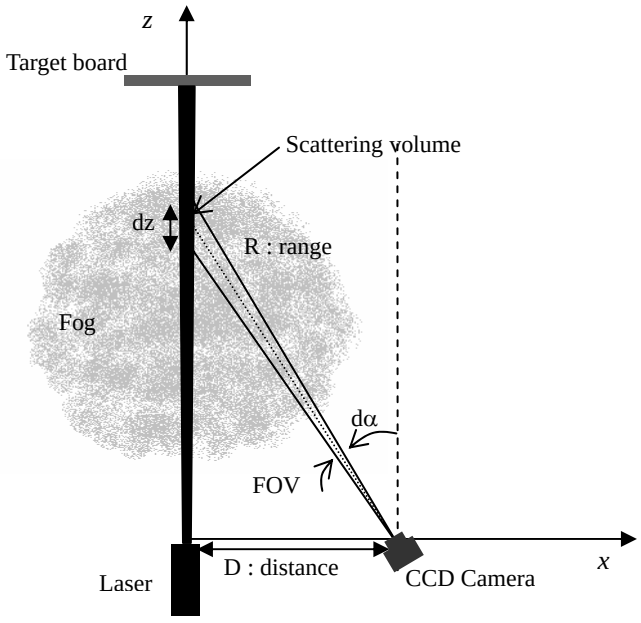

Fig. 4. The geometry of a bistatic lidar.

Therefore, in our case Eq. (1) becomes [8]

$$P_r = P_t \frac{KAT^2 \beta(z,\theta)}{D} d\alpha \ . \tag{3}$$

The cancellation of the R^2 dependence has the important consequence that the detector is not required to have a large dynamic range for signal detection.

In our experiments, the effects of multiple scattering of narrow light beams propagating in aerosols are investigated using two particular features; the radial distribution of scattered light and the angular change of polarization ratio compared with single particle scattering. The radial distribution of multiply scattered light as a function of optical depth was examined previously by Bissonnette [9]. It was found that the central part of the transmitted beam, which has its Gaussian shape, is not affected by multiple scattering. The transmitted beam extinction along the direction of beam propagation is governed by Beer-Lambert's law. The narrow central part of the beam is surrounded by a wider aureole, which is due to multiple scattering and its size increases with optical depth.

Polarization ratio is also a useful parameter because spatial and temporal aerosol number density variations in measurements made at different scattering angles are cancelled out [10]. Pal and Carswell [11] were among the first to experimentally study the variation of the polarization ratio, δ_p , associated with scattering from homogeneous spheres. In mathematical form, the polarization ratio is given by

$$\delta_p = \frac{I_{//}(\theta)}{I_{\perp}(\theta)} \ , \tag{4}$$

where $I_{//}(\theta)$ is scattered intensity from incident parallel polarization, $I_{\perp}(\theta)$ is scattered intensity from incident perpendicular polarization. Depolarization can be caused by the polarization anisotropy of atmospheric molecules, nonsphericity of particle, or by multiple scattering. However, the depolarization component from the atmospheric molecules is generally small [12] and that from nonspherical particles is ignored in our experiments because it can be assumed that the oil fog in the chamber experiments and the natural water fog in the field tests are consisting of nearly spherical particles. Therefore, a reasonable assumption is that the primary source of depolarization is multiple scattering.

4 RESULTS

The Monte Carlo calculations were performed using four models of fog and cloud aerosols and the experimental results are presented in this section.

4.1 Bistatic Monte Carlo simulation

There are many examples of using Monte Carlo methods to simulate the interaction between light and atmospheric particles for a conventional monostatic lidar geometry [13]. However, there only appears one computer simulation program for a bistatic lidar geometry. The Bistatic Monte Carlo (BMC) program developed by Sergei M. Prigarin has, with modifications needed for our application, proven to provide successful simulations for our bistatic lidar system.

Three fog models are chosen to simulate multiple scattering, and a haze M model is also included for comparisons with our measurements, and with the case of single particle scattering from small particles. The particle size distributions of each model used are described by a modified Γ-distribution which can be used to represent various types of

realistic aerosol distributions of rain and water clouds [14,15],

$$\frac{dn(r)}{dr} = ar^{\alpha} \exp(-br^{\gamma}) \quad , \tag{5}$$

where $n(r)$ is the number density of particles with radii between r and $r+dr$. By assigning different values to the parameter α and γ one can obtain different atmospheric aerosol model conditions. The important parameters of each model used in our simulations are tabulated in Table 2. Scattering phase functions, which are the input parameter for the simulations of each model, are also shown in Fig. 5.

Our simulation consists in calculating the expected returns from the two polarization orientations of the laser beam scattering from a 36 m thick aerosol medium. The selected lidar geometry for the simulations is similar to that of the chamber and field experiments. The scattering medium is at a distance of 100 m from the laser and the atmosphere in front of the scattering is assumed to neither absorb nor scatter. The wavelength of a pulsed laser is 532 nm and the beam divergence is equal to 0.2 mrad full angle. The pulse length is 5 ns. The refractive index of each scattering medium is taken as $m = 1.325 + 0i$.

Table 2. Parameters for the particle size distribution [16].

Model type	a	α	b	γ	r_e (μm)	N_0 (cm^{-3})
Heavy advective fog	0.027	3	0.3	1.0	10.0	20
Moderate advective fog	0.066	3	0.375	1.0	8.0	20
Heavy radiation fog	2.373	6	1.5	1.0	4.0	100
Haze M	$16/3 \cdot 10^5$	1	8.943	0.5	0.05	100

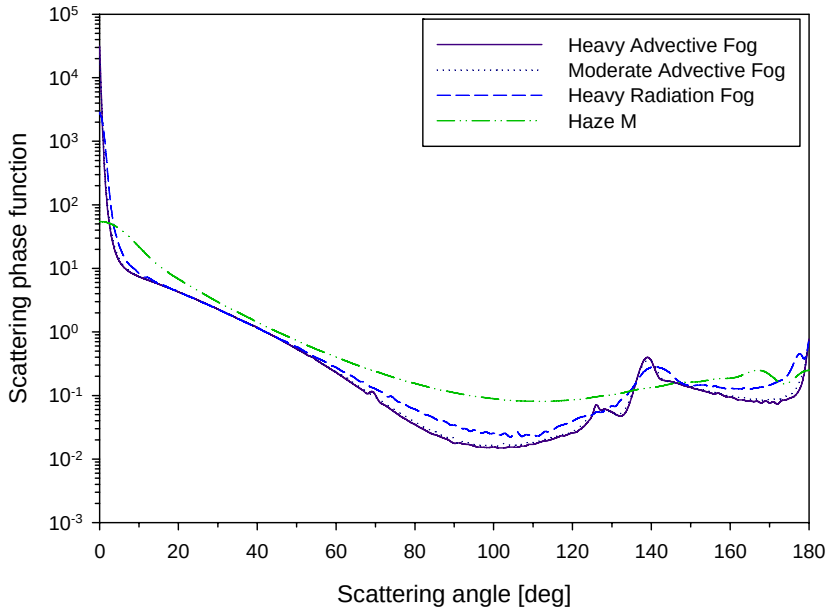

Fig. 5. Scattering phase functions for single particle scattering for the aerosol models used in the BMC simulation.

The field of view of a detector is 840 mrad (48°). In each case, a single scattering albedo is assumed to be one, which means absorption by atmospheric particles is not considered in our calculations. Lidar returns are plotted for both forward and backward directions. For comparison with single scattering calculations using the Mie theory, the scattering phase function for single particle scattering is also included in each plot. One can then easily see the difference of angular distribution of multiply scattered light caused of different size distributions and optical depths, as depicted in the results shown in Fig. 6. The symbols present the BMC calculations and the curve represents the Mie calculation from single scattering. In all cases, single scattering component follows scattering phase function very well between 0° and 20° in the forward direction and 160° and 180° in the backward direction. However, it starts deviating from single scattering phase function at the scattering angles bigger than 20° and smaller than 160° due to the increase of multiple scattering. The intensity of multiple scattering increases as the extinction coefficient increases over the entire angular region of interest. In case of a heavy advective fog (σ_{ext} = 0.03 m^{-1}), the intensity of multiple scattering is comparable to or bigger than that of single scattering. However, in case of the small particle size distribution of the haze M model (σ_{ext} = 0.001 m^{-1}), single scattering dominates.

Simulations are also performed to investigate atmospheric conditions when aerosol multiple scattering processes are significant. The lidar returns of single and multiple scattering are plotted on a log-scale of optical depth. As shown in each lidar-return plot, optical scattering in all models is meaningful in optical depth up to 10, which means that the transmitted laser beam is totally attenuated by scattering media after this point. Calculations of multiple scattering from atmospheric volumes having large particles (fog models) show increasing contributions due to multiple scattering from an optical depth of 0.1 and shows a maximum contribution between 0.3 and 0.7. However, in the case of the Haze M model, which has an effective radius smaller than the incident wavelength, the multiple scattering effect is negligible for optical depths in the range 0.1-10. Another important aspect realized from these results is that multiple scattering contributions are comparable to single scattering at optical depths near 1. At this optical depth, the penetration distance is almost the same (ie. about 30 m) in each of these fog models. However, in the case of Haze M model, single scattering is dominant up to the penetration distance of 4 km. The results are shown in Fig. 7.

4.2 Experimental results

Experimental results of chamber tests and field tests are presented in this section. The data analysis is focused on the data from forward and backward directions. From the data obtained in the forward direction, a radial distribution of multiply scattered radiation is mainly analyzed. In the backward direction, the polarization ratios are calculated as a function of scattering angle.

Good agreement is shown with Bissonnette's result [8] and our measurements obtained with from a multistatic lidar. Fig. 8 shows the CCD image of a laser beam propagation in fog, which was taken in the field tests. Each vertical white line represents the position where the data were analyzed. It is clearly shown that the unscattered narrow beam continues far into the scattering medium but it is surrounded by a halo which has the geometry of a forward beam although much wider due to multiple scattering. The data in Fig. 9 (a) are analyzed from Fig. 8. As the optical depth increases, the ratio of the multiple-to-single scattering contribution also increases. For comparison, the radial distribution measured at clear night, which is single-scattering-dominant atmospheric condition, is also shown in Fig. 9 (b). In this case, the multiple scattering components (aureole parts) are very small compared to that of single scattering and do not change with different optical depths.

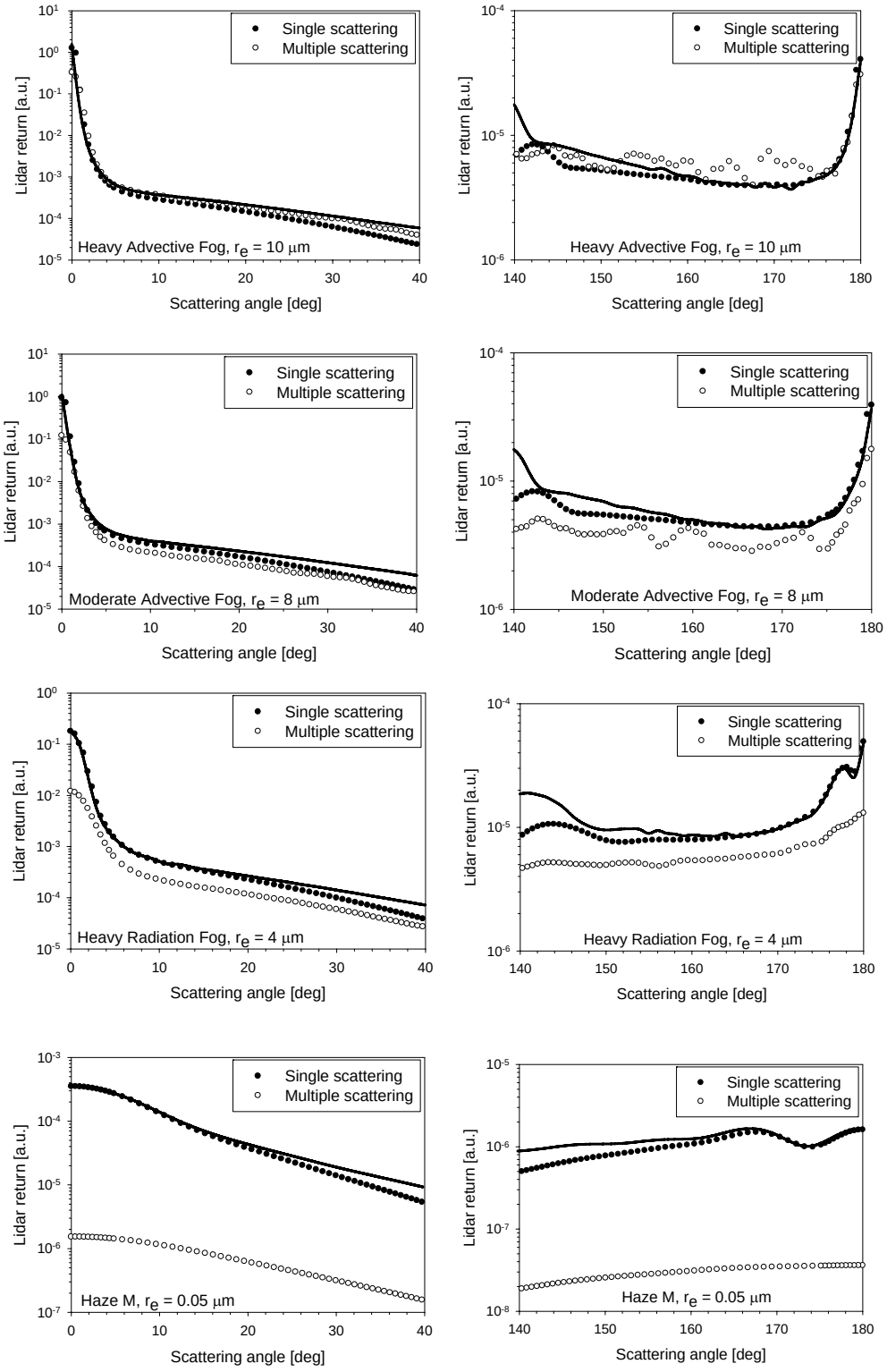

Fig. 6. Angular distributions of multiply scattered radiation of four different models.

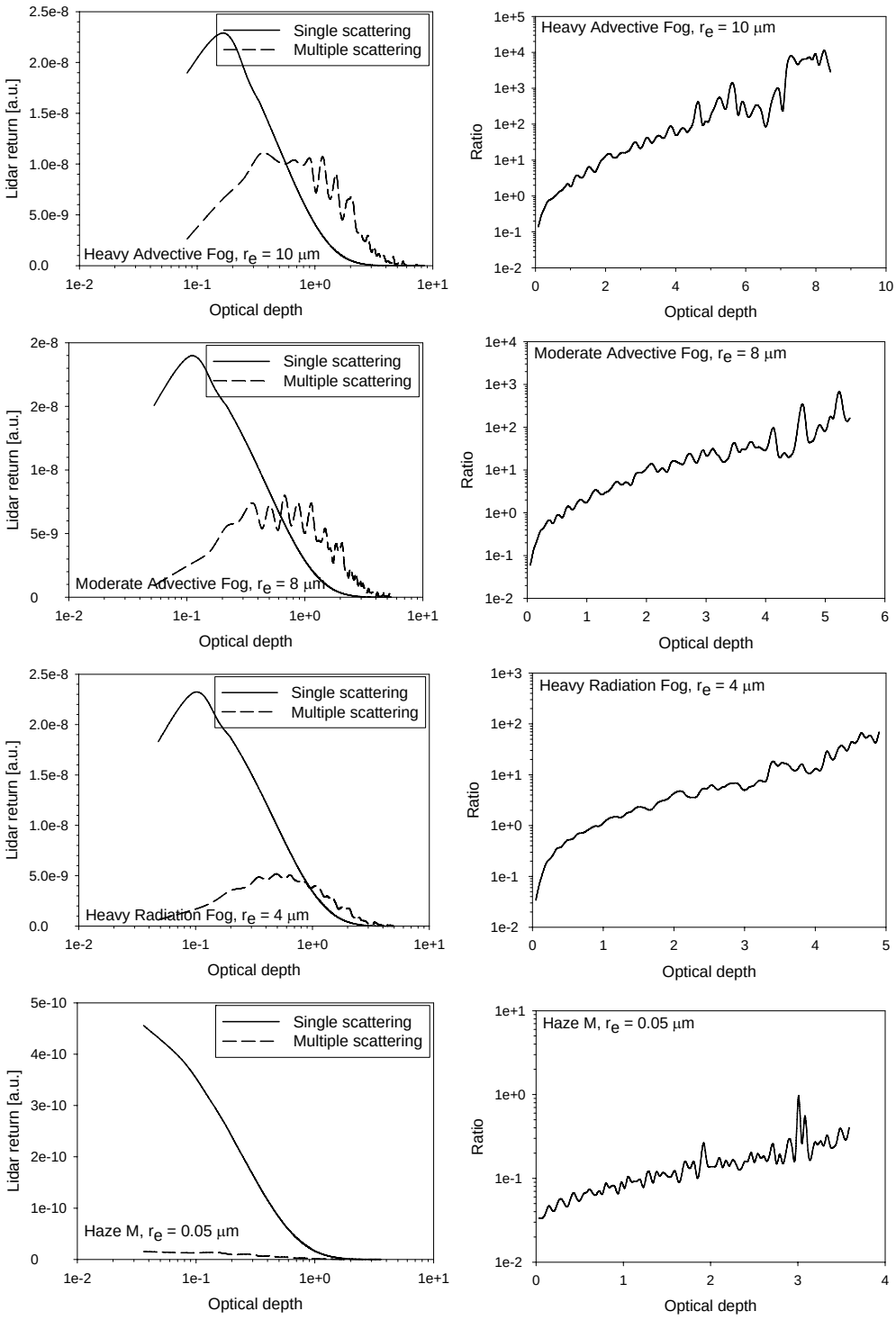

Fig. 7. Lidar returns and calculated ratios of the multiple-to-single scattering contributions of four different models.

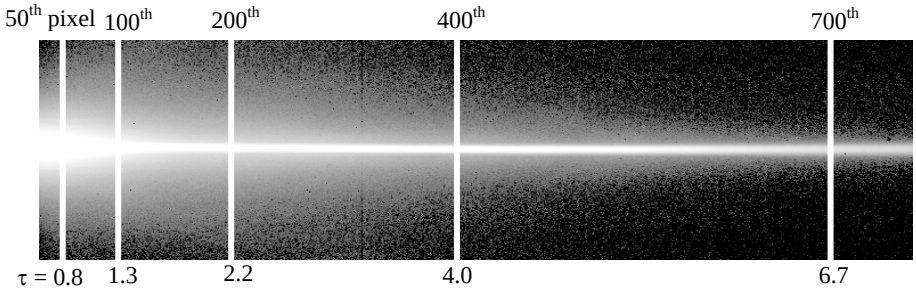

Fig. 8. CCD image of a laser beam propagation through fog measured at field tests.

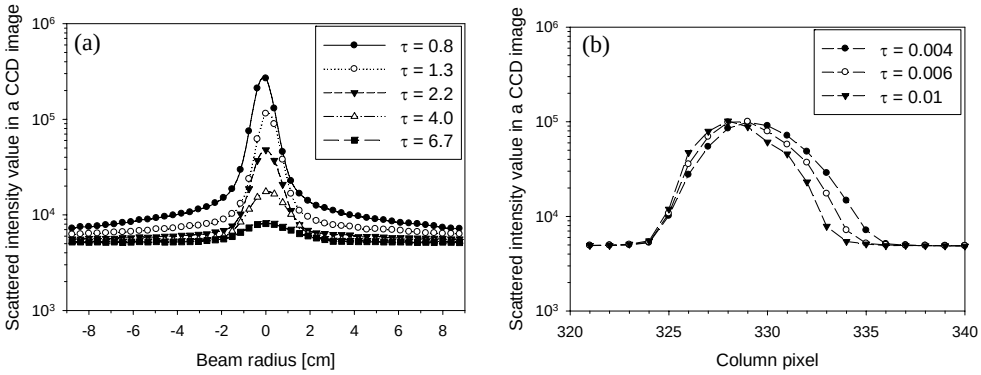

Fig. 9. Radial distributions of scattered radiation measured at (a) foggy night and (b) clear night.

The locations of the maximum intensity are not perfectly matched with each other simply due to the misalignment of the laser beam in the horizontal direction in a CCD image.

Polarization ratios measured on clear and foggy nights are presented in Fig. 10. The circle symbols present polarization ratios of single scattering in the laser beam while the triangle symbols present that of multiple scattering. In the case of a clear night (σ_{ext} = 0.0002 m^{-1}), the difference of polarization ratio between single and multiple scattering is not distinguishable, which means that single scattering is dominant process. However, in the case of a foggy night (σ_{ext} = 0.1 m^{-1}), the polarization ratio of multiple scattering increases in the entire scattering angle of interest and approaches that of single scattering at larger scattering angles. This is because the phase function at scattering angles, $\theta > 160°$, both polarization components begin to develop the same backscattering enhancement. This phenomenon is also seen in the BMC simulation.

5 CONCLUSIONS

Using the multistatic lidar and the measurements of radial distribution of scattered radiation and polarization ratio, multiple scattering can be distinguished from single scattering over different angular regions. Numerical simulations using the Bistatic Monte Carlo (BMC) method were performed. Radial distribution of scattered radiation from the multistatic lidar can be easily analyzed from a CCD image and shows the spatial characteristics of multiple scattering along the beam path. The changes in the radial distribution of multiple scattering are related to the extinction coefficient, or the size/number density, given in terms of optical depth within the scattering volume.

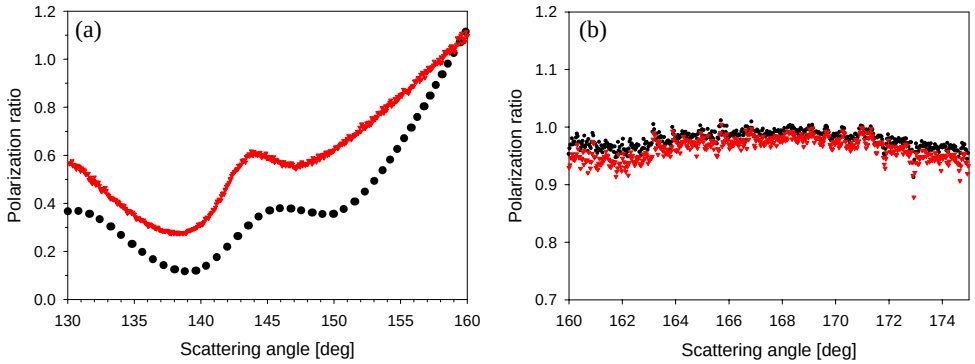

Fig. 10. Polarization ratios measured at (a) foggy night and (b) clear night.

Polarization ratio of the scattering phase function at different scattering angles also provided a way to extract multiple scattering effects from the multistatic lidar. Multiple scattering increases the depolarization of the scattered radiation at side-scattering region.

Acknowledgements

We would like to thank the researchers at Defense Research and Development Canada for the opportunity to use the DRDC facilities. We would also like to thank Sergei M. Prigarin for allowing us to use the Bistatic Monte Carlo program.

References

[1] Ben Veihelmann, Martin Konert, and Wim J. van der Zande, "Size distribution of mineral aerosol: using light-scattering models in laser particle sizing", *Appl. Opt*., Vol. 45, 6022-6029 (2006).

[2] Gilles Roy, Luc Bissonnette, Christian Bastille, and Gilles Vallee, " Retrieval of droplet-size density distribution from multiple-field-of-view cross-polarized lidar signals: theory and experimental validation", *Appl. Opt*., Vol. 38, 5202-5211 (1999).

[3] Jin H. Park and C. R. Philbrick, "Multiple scattering measurements Using Multistaic Lidar," *2006 International Aerosol Conference*, Vol. 1, 703-704 (2006).

[4] M. I. Mishchenko, L. D. Travis, and A. A. Lacis, *Scattering, Absorption, and Emission of Light by Small Particles*, Ch. 10, Cambridge, New York (2002).

[5] E. J. Novitsky, "Multistatic Lidar Profile Measurement of Lower Troposphere Aerosol and Particulates", PhD Thesis, The Pennsylvania State University (2002).

[6] C. R. Philbrick, M. D. O' Brian, D. B. Lysak, T. D. Stevens, and F. Balsiger, "Remote sensing by active and passive optical techniques, NATO/AGARD Proceedings on Remote Sensing, "*AGARD Conf. Proc*., 582, pp. 8.1-8.9 (1996).

[7] T. D. Stevens, "Bistatic Lidar Measurements of Lower Tropospheric Aerosols," Ph D Thesis, The Pennsylvania State University (1996).

[8] K. Meki, K. Yamaguchi, X. Li, Y. Saito, T. D. Kawahara, and A. Nomura, "Range-resolved bistatic imaging lidar for the measurement of the lower atmosphere", *Opt. Lett*., Vol. 21, No. 17, 1318-1320 (1996).

[9] L. R. Bissonnette, "Multiple scattering of narrow light beams in aerosols", *Appl. Phys*., Vol. 60, 315-323 (1995).

[10] J. A. Reagan, D. M. Byrne, and B. M. Herman, "Bistatic lidar: a tool for characterizing particulates. Part 1. The remote sensing problem", *IEEE Trans. Geosci. Remote Sens*., 229-235 (1982).

[11] S. R. Pal and A. I. Carswell, “Polarization Properties of Lidar Backscattering from Clouds”, *Appl. Opt*., Vol. 12, 1530-1535 (1973).
[12] A. T. Young, “Rayleigh Scattering”, *Phys. Today*, Vol. 35, 42-48 (1982).
[13] L. R. Bissonnette, P. Bruscaglioni, A. Ismaelli, G. Zaccanti, A. Cohen, Y. Benayahu, M. Kleiman, S. Egert, C. Flesia, P. Schwendimann, A. V. Starkov, M. Noormohammadian, U. G. Oppel, D. M. Winker, E. P. Zege, I. L. Katsev, and I. N. Polonsky, “LIDAR multiple scattering from clouds”, *Appl. Phys*., Vol. 60, 355-362 (1995).
[14] Luc R. Bissonnette, Gilles Roy, and Nathalie Roy, “Ground-based lidar measurement of liquid water content and effective droplet diameter in water clouds: instrumentation, retrieval method and results”, *Proc. of SPIE*, Vol. 5235, 537-548 (2004).
[15] Yonxiang Hu, Zhaoyan Liu, David Winker, Mark Vaughan, and Vincent Noel, “Simple relation between lidar multiple scattering and depolarization for water clouds”, *Opt. Lett*., Vol. 31, 1809-1811 (2006).
[16] Christian Werner, Jurgen Streicher, Ines Leike, and Christph Munkel, “Visibility and Cloud Lidar” in *Lidar Range-Resolved Optical Remote Sensing of the Atmosphere*, Ch. 6, Springer, New York (2005)

Jin H. Park is a graduate student at the Pennsylvania State University. He received has BS degree in physics from the Korea Military Academy in 1995 and MS degree in electrical engineering from the University of Pittsburgh in 2000, respectively, and is pursuing his PhD degree in the Pennsylvania State University. His current research interests include optical scattering in atmosphere and remote sensing.

C. Russell Philbrick, Ph.D., earned BS 1962, MS 1964, and PhD 1966 degrees in Physics from N.C. State University while performing early laser investigations. He was with the Air Force Cambridge Research Laboratory (now AFRL) for 21 years in where he developed rocket, satellite, and remote sensing techniques for investigations of the composition, structure, and dynamics of the atmosphere and ionosphere. Dr. Philbrick joined Penn State University in 1988 as Professor of Electrical Engineering and lectures in areas of optics, space physics, electromagnetics, and laser remote sensing. For the past 30 years, his group has developed and improved many lidar techniques, while using lidar for investigations sponsored by DoD, NSF, EPA, DOE, and other agencies. He has served as principal advisor for graduate degrees of more than 50 students, several senior honors theses, and for several student projects that prepared and launched instruments on space shuttle flights, rockets, and satellites.